RAA 2015 Vol. **15** No. **2**, 199–206 doi: 10.1088/1674–4527/15/2/004
http://www.raa-journal.org *http://www.iop.org/journals/raa*

Research in Astronomy and Astrophysics

Possible evidence of destroying small PAH particles by radiation from AGNs *

Qi-Chen Feng[1,2], Jing Wang[1] and Jian-Yan Wei[1]

[1] National Astronomical Observatories, Chinese Academy of Sciences, Beijing 100012, China; *fqch@bao.ac.cn*
[2] University of Chinese Academy of Sciences, Beijing 100049, China

Received 2014 April 23; accepted 2014 June 3

Abstract The issue of destroying small polycyclic aromatic hydrocarbon (PAH) particles by radiation from AGNs is examined through optical narrow-emission line ratios of a sample of type II AGNs. We find that narrow-line ratios [OI]λ6300/Hα and [SII]λ6716, λ6731/Hα have prominent correlations with the PAH 11.3/7.7 ratio in our selected sample of AGNs. Because of the marginal (and in some cases no) dependence of the PAH ratio on the gas metallicity, a possible explanation for the correlations is the destruction of small PAH particles by the hard ionizing field associated with the AGNs.

Key words: infrared: ISM — quasars: emission lines — galaxies: active — galaxies: AGN — methods: statistical

1 INTRODUCTION

Polycyclic aromatic hydrocarbons (PAHs) are a kind of aromatic molecule everywhere in the interstellar medium (ISM) of the Milky Way and most nearby galaxies that have ongoing or recent star formation. Generally, PAHs are considered to be the most efficient species that undergo photoelectric heating (Bakes & Tielens 1994) in photodissociation regions (PDRs). PAHs are stochastically heated by ultraviolet (UV) and optical photons that predominantly originate from massive stars and then the incident energy is re-emitted in the infrared band. The luminosity in the mid-IR PAH emission bands is very strong for galaxies with ongoing or recent star formation. In galaxies with intense star formation, up to 20% of the total infrared luminosity is emitted in the PAH bands alone (Smith et al. 2007b).

PAH emission has been seen in many environments, including stars, HII regions, the ISM, nebulae, PDRs as well as whole galaxies. This phenomenon has been extensively observed by the *Infrared Space Observatory* and was recently investigated with higher sensitivity using the *Spitzer* Space Telescope (Verma et al. 2005; Smith et al. 2007b). Because of heating by the UV and optical photons from a massive star, PAH emission is widely used to estimate the star formation rate (Roussel et al. 2001; Dale & Helou 2002) in star-forming regions (Genzel et al. 1998; Clavel et al. 2000).

There are four prominent PAH features in the mid-infrared from 5 to 19 μm, at 6.2, 7.7, 11.3 and 17 μm. The total power emitted in these PAH lines is significant, especially because the 7.7 μm

* Supported by the National Natural Science Foundation of China.

PAH feature accounts for nearly 50% of PAH luminosity in all and about 10% of the total infrared luminosity (Smith et al. 2007b).

The fraction of power radiated by PAHs in the different bands depends on both PAH ionization and the size of a PAH grain (Draine & Li 2007). Thus, the observed variations in the band-to-band ratios from PAHs can reflect variations in physical conditions (Smith et al. 2007b; Galliano et al. 2008; Gordon et al. 2008; O'Dowd et al. 2009). They show a higher $G_0/n_{\rm e}$ (G_0 is the intensity of the incident UV radiation field and $n_{\rm e}$ is the electron density) ratio that favors a larger fraction of positively ionized PAHs (Bakes et al. 2001).

Previous studies with the *Spitzer* Space Telescope (Diamond-Stanic & Rieke 2010; O'Dowd et al. 2009; Smith et al. 2007b) have found trends between the ratios of the various PAH features and properties of galaxies, such as AGN activity and star formation history. AGN-dominated sources tend to have a lower PAH 7.7/11.3 ratio than star-forming galaxies, possibly due to the preferential destruction of smaller aromatics by the AGN's accretion power (Wu et al. 2010). Smith et al. (2007b) argued that AGNs are able to modify the PAH grain size distribution (by shocks or X-ray emission associated with the AGNs) or are able to excite large PAH molecules. In other words, the difference in the PAH's luminosity ratio comes from differences between the energy spectral index in AGNs and star-forming galaxies.

If the above scenario is correct, one expects to see a dependence of the PAH feature ratio on the spectral slope of AGNs at high energy. In this paper, the dependence is studied by using the optical emission line ratios [OI]λ6300/Hα and [SII]λ6716, 6731/Hα from a sample of AGNs, since the two line ratios are mainly determined by the hardness of the ionizing field associated with an AGN (Kewley et al. 2006; Wang & Wei 2008). Type II AGNs are the focus of the sample in this study just because the narrow-line ratios are easy to measure in their optical spectra. This paper is organized as follows. The sample is described in Section 2; we give the results and discussion in Section 3. The last section is a short summary.

2 SAMPLE

We compile a sample of type II AGNs with the measured PAH features at 7.7 and 11.3 μm from the literature. All the fluxes of both features were measured from the spectra taken by the low-resolution and high-resolution *Spitzer* Infrared Spectrograph (IRS; $\lambda = 5.2 \sim 14.5$ μm, $R = 64 \sim 128$, Houck et al. 2004). The one-dimension spectra were extracted by CUBISM (Smith et al. 2007a) from the basic calibrated data using $3.6'' \times 7.2''$ apertures oriented along the slit direction. The fluxes of the 7.7 and 11.3 μm features were then modeled by PAHFIT, a spectral decomposition routine that models the dust continuum, starlight continuum, unresolved emission lines, PAH emission features and silicate absorption/emission (Smith et al. 2007a). For each object, the corresponding optical narrow line fluxes were taken from a variety of previous studies. The sample finally contained 29 nearby ($z = 0.002 \sim 0.029$) type II AGNs, and the infrared PAH ratios and optical line ratios are listed in Table 1.

The sample is located on the three Baldwin-Phillips-Terlevich (BPT) diagrams in Figure 1. The BPT diagrams are powerful tools to determine the dominant energy source in narrow emission-line galaxies (Baldwin et al. 1981; Veilleux & Osterbrock 1987). AGNs are concentrated in the upper right corner of the three BPT diagrams, because of their stronger and harder ionizing field. The solid line in each panel shows the theoretical demarcation line that distinguishes "pure" AGNs from star-forming galaxies (Kewley et al. 2001). The dashed line in the [NII]/Hα versus [OIII]/Hβ diagram is the empirical demarcation line proposed by Kauffmann et al. (2003), which is widely used to separate "pure" star-forming galaxies according to data from the Sloan Digital Sky Survey. Figure 1 indicates that all the objects listed in the current sample are located above the empirical line, and more than 90% of the objects can be classified as "pure" AGNs according to the Kewley demarcation lines.

Table 1 The Optical Emission Line Ratios and PAH 11.3/7.7 Ratios in the Sample of Type II AGN Galaxies

Name	z	PAH 11.3/7.7	[OIII]/Hβ	[OI]/Hα	[NII]/Hα	[SII]/Hα	[OI]/[NII]	12+log(O/H)$_{\rm SSCK1}$	Reference
NGC 1144	0.029	0.358	7.1	0.234	0.84	0.832	0.279	8.573	[1, 2, 3, 4]
NGC 1320	0.009	0.253	8.98	0.126	0.708	0.417	0.178	8.571	[1, 3, 5]
NGC 5953	0.0066	0.304	2.968	0.06	0.78	0.4	0.077	8.512	[1, 6, 7]
MRK3	0.014	0.0859	13.37	0.13	0.61	0.3	0.213	8.632	[8, 10]
MRK1066	0.012	0.2618	3.89	0.0933	0.871	0.389	0.107	8.539	[3, 5, 8]
NGC 3690	0.01	0.247	1.37	0.031	0.4	0.25	0.078	8.425	[9, 11]
NGC 1058	0.002	0.397	3.81	0.18	1.23	0.73	0.146	8.612	[11, 12]
NGC 2992	0.008	0.229	8.149	0.129		0.671		8.367	[6, 12, 13]
NGC 3735	0.009	0.224	7.14	0.053	0.85	0.38	0.062	8.576	[11, 12]
NGC 5395	0.012	0.498	3.03	0.17	1.23	0.76	0.138	8.603	[11, 12]
NGC 1386	0.003	0.19	10.73	0.105	1.188	0.484	0.088	8.733	[1, 14]
NGC 1667	0.015	0.303	7.58	0.24	0.691	0.42	0.347	8.544	[1, 11, 15]
NGC 4501	0.008	0.606	4.528	0.19	1.86	0.94	0.102	8.74	[1, 4, 11, 16]
NGC 5135	0.014	0.230	6.607	0.074	0.813	0.346	0.091	8.559	[12, 17 ,18]
NGC 5194	0.002	0.429	6.176	0.167	2.4	0.58	0.069	8.865	[1, 4, 19, 20]
NGC 5929	0.008	0.475	3.42	0.263	0.68	0.59	0.387	8.495	[1, 2, 3, 19]
NGC 7172	0.009	0.169	10	0.117	0.3	0.513	0.392	8.475	[1, 2, 4, 18]
NGC 7674	0.029	0.195	8.318	0.0501	0.64	0.324	0.078	8.542	[1, 3, 4, 21]
NGC 4945	0.002	0.088			0.3	0.15		8.403	[22, 27]
NGC 2273	0.006	0.291	5.77	0.12	0.86	0.47	0.14	8.558	[11, 12]
NGC 3079	0.004	0.157	4.169	0.0578	1.585	0.434	0.036	8.684	[3, 5, 12, 23]
NGC 3185	0.004	0.285	3.42	0.045	0.75	0.37	0.06	8.51	[11, 12, 19]
NGC 3227	0.004	0.324	5.91	0.13	1	0.68	0.13	8.591	[10, 11, 12]
NGC 5427	0.009	0.239	8.1	0.261	1.622	0.513	0.161	8.768	[12, 13, 18, 19]
NGC 5643	0.004	0.447	11.4	0.186	1.0383	0.708	0.179	8.71	[3, 12, 14]
NGC 6221	0.005	0.215	0.647	0.018	0.652	0.22	0.028	8.475	[6, 12, 13, 15]
NGC 6951	0.005	0.319	6.62	0.23	2.455	0.91	0.094	8.885	[11, 12, 24]
NGC 7496	0.006	0.219	0.655	0.043	0.457	0.221	0.095	8.435	[12, 15, 17, 25]
NGC 7590	0.005	0.377	5	0.11	1.05	0.539	0.105	8.59	[2, 12, 15, 26]

References: [1] LaMassa et al. (2012); [2] Wu et al. (2011); [3] Yu & Hwang (2011); [4] LaMassa et al. (2010); [5] Yu et al. (2013); [6] Gu et al. (2006); [7] Dudik et al. (2009); [8] Sales et al. (2010); [9] Pereira-Santaella et al. (2010); [10] Winter et al. (2010); [11] Ho et al. (1997); [12] Diamond-Stanic & Rieke (2010); [13] Veron-Cetty & Veron (1986); [14] Bennert et al. (2006); [15] Storchi-Bergmann et al. (1995); [16] Shields et al. (2007); [17] Vaceli et al. (1997); [18] Lumsden et al. (2001); [19] Keel et al. (1985); [20] Heckman et al. (1980); [21] Ashby et al. (1995); [22] Goulding & Alexander (2009); [23] Tran (2003); [24] Seth et al. (2008); [25] Kewley et al. (2000); [26] Shi et al. (2010); [27] Dudik et al. (2009).

3 RESULTS AND DISCUSSION

Figures 2 and 3 present strong correlations between [SII]/Hα and [OI]/Hα with the PAH 11.3/7.7 ratio. A Kendall test returns a correlation coefficient of $\tau = 0.5345$ at a significance level of $p < 10^{-4}$ for the [SII]/H$\alpha - 11.3/7.7$ ratio relation, where p is the probability that there is no correlation between the two variables. The same test applied to [OI]/Hα returns $\tau = 0.3942$ ($p = 0.0032$). Compared to [SII]/Hα, the lower significance for the [OI]/Hα–PAH 11.3/7.7 correlation could be due to the lower signal-to-noise ratio of [OI]/Hα emission lines.

The previous studies indicate that these two optical narrow-line ratios in AGNs are related to both the ionization hardness and the metallicity of the gas. Stasińska (1984) investigated the consequences of the change in the spectral index α of the assumed photoionizing power-law spectrum $\nu^{-\alpha}$ on these two line ratios. As α becomes smaller, the ionization by X-ray photons becomes more important and both [OI]/Hα and [SII]/Hα become larger. The same correlation was obtained by

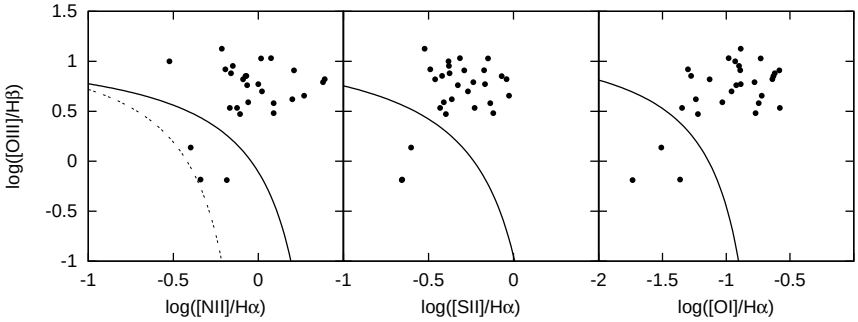

Fig. 1 The BPT designations. The solid line shows the theoretical demarcation line that distinguishes "pure" AGNs from star-forming galaxies (Kewley et al. 2001). The dashed line in the [NII]/Hα versus [OIII]/Hβ diagram is the empirical demarcation line proposed by Kauffmann et al. (2003), which is widely used to separate "pure" star-forming galaxies.

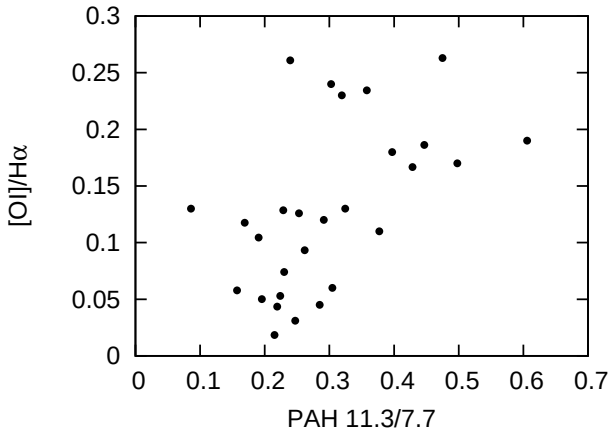

Fig. 2 [OI]/Hα vs. the PAH 11.3/7.7 ratio; a positive correlation can be seen.

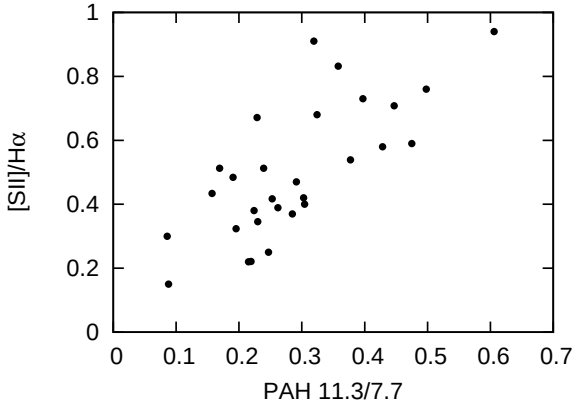

Fig. 3 [SII]/Hα vs. the PAH 11.3/7.7 ratio; a positive correlation can be seen.

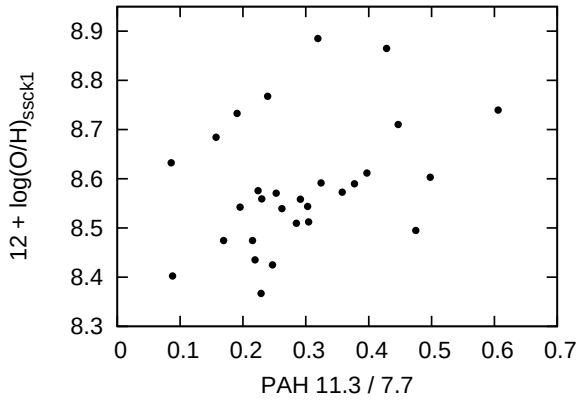

Fig. 4 PAH 11.3/7.7 vs. $12+\log(\mathrm{O/H})_{\mathrm{SSCK1}}$; $12+\log(\mathrm{O/H})_{\mathrm{SSCK1}}$ represents the gas metallicity of narrow-line regions in AGNs. There is a marginal dependence between the metallicity and the PAH 11.3/7.7 ratio.

Kewley et al. (2006) through their photoionization simulations. In addition, Wang et al. (2013) recently reported a direct correlation between these two narrow-line ratios and the spectral slope of AGNs at high energy.

From Figures 2 and 3, we can connect the correlation between the ratio of PAH 11.3/7.7 and the index α in the power-law spectra of AGNs. The result probably agrees with our expectation, which indicates the dependence of PAH feature ratios on the spectral slope of AGNs at high energy. This means that the harder the radiation field that exists, the larger the 11.3/7.7 ratio becomes. The role of hard radiation from the AGN on the PAH feature ratio has been comprehensively examined in previous studies.

The two line ratios could be additionally effected by the gas metallicity. Storchi-Bergmann et al. (1998) provided us with the SSCK method for calibration of the gas metallicity of narrow-line regions in AGNs

$$\begin{aligned} 12+\log(\mathrm{O/H})_{\mathrm{SSCK1}} \;=\; & 8.34+0.212x-0.012x^2-0.002y+0.007xy-0.002x^2y \\ & +6.52\times10^{-4}y^2+2.27\times10^{-4}xy^2+8.87\times10^{-5}x^2y^2\,, \end{aligned} \quad (1)$$

where $x \equiv$[NII]λ6583/Hα and $y \equiv$[OIII]λ5007/Hβ.

We can see the result of this metallicity test in Figure 4. There is a very marginal dependence between the metallicity and the PAH 11.3/7.7 ratio. We obtain a similar result by using the [OI]/[NII] ratio instead of the SSCK method (Nagao et al. 2002) in Figure 5. Therefore, the metallicity is not an important issue that affects the PAH 11.3/7.7 ratio.

Smith et al. (2007b) divided their sample into two groups and found that the PAH 11.3/7.7 ratio of the low-luminosity AGN group had increased rapidly corresponding to hardness ratios [NeIII]/[NeII] being stronger. However, the PAH feature ratio of the other HII-type galaxy group was constant. The observed increase in the PAH 11.3/7.7 ratio suggested there was selective destruction of those PAHs that was small enough to emit at 7.7 μm. Other studies have also shown there are positive correlations in the [NeIII]/[NeII] versus PAH 11.3/7.7 ratios. Those facts could be used to conclude that galaxies with an increasing hardness in the radiation fields from an AGN have relatively less emission from PAH features at shorter wavelengths compared to PAH features at longer wavelengths (O'Dowd et al. 2009; Wu et al. 2010). In other words, harder radiation fields are more efficient at destroying small PAH grains; that effect may dominate the center of the galaxies. It is

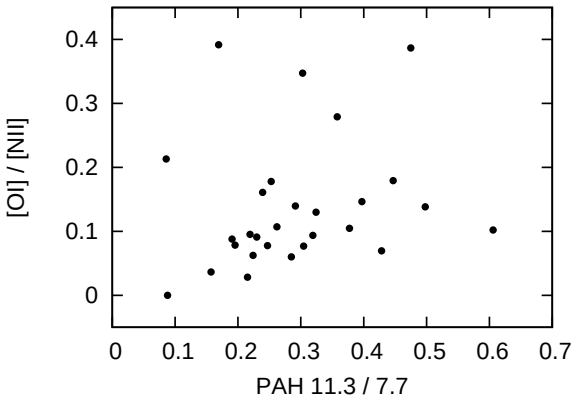

Fig. 5 PAH 11.3/7.7 vs. [OI]/[NII]; [OI]/[NII] represents the gas metallicity of narrow-line regions in AGNs. There is no correlation between the [OI]/[NII] ratio and the PAH 11.3/7.7 ratio.

consistent with the possibility that an AGN can emit X-rays with sufficient energy to destroy smaller PAHs even at distances of kiloparsecs, where larger ones are harder to destroy (Voit 1992).

All the previous research revealed the fact that the PAH ratio depends on the difference in the spectral index (slope) of the physical object. The PAH ratios could be used to discriminate normal galaxies from AGNs. Our study takes one step further: to differentiate types of AGNs. The result suggests that a smaller α (harder X-ray) leads to more effective destruction of the 7.7 μm PAH band. It also confirms the lab experiment that a small PAH is easily destroyed in the environment of a similar Type II AGN (Voit 1991).

Pereira-Santaella et al. (2010) show the 7.7 μm PAH emission may be produced in star-forming regions, but the 11.3 μm PAH emission also comes from diffuse regions. Thus, low values of the PAH 11.3/7.7 ratio trace HII regions, which are associated with the brightest PAH emission (Galliano et al. 2008), and larger values indicate less recent star formation. We should notice that the optical line ratios have a significant correlation with $D_n(4000)$, in which the value means "age" of the host galaxies and larger line ratios correspond to older stellar populations (Wang & Wei 2008, 2010). Therefore, our results indicate that the PAH 11.3/7.7 ratio tends to be larger among older "age" host galaxies. This is consistent with the link between the status of a PAH feature ratio for an AGN and the age of the stellar population (O'Dowd et al. 2009).

However, the 11.3/7.7 band intensity ratio can also be affected by the PAH ionization state (Tielens 2008). The ratio of ionized PAH 7.7 particles to neutral PAH 11.3 grains is set by the balance between ionization and recombination, which depends on the UV incident radiation field density (G_0), the gas temperature (T) and the electron density ($n_{\rm e}$) according to $G_0T^{1/2}/n_{\rm e}$ (Bakes & Tielens 1994). In order to distinguish the contribution from changes in the ionized fraction of PAHs or changes in PAH size, we examined the 6.2/7.7 ratios of this sample, which could be a better indicator of PAH size (Draine & Li 2001). We obtained the only 18 PAH 6.2/7.7 ratios left in the selection sample and found there is basically no obvious relations between the PAH 6.2/7.7 ratio and [OI]/Hα as well as the PAH 6.2/7.7 ratio and [SII]/Hα. One possible explanation could be that the PAH molecules emitting the 6.2 μm and 7.7 μm features are destroyed with similar efficiency due to the average sizes of molecules (O'Dowd et al. 2009). Therefore, we cannot completely rule out the possibility that the variations in the 11.3/7.7 ratio are caused by the ionization state.

4 SUMMARY

We selected a sample of narrow emission line galaxies to explore the effect of AGN radiation on the PAH 11.3/7.7 ratio. The three BPT diagrams confirm that our sample targets ($> 90\%$) are "pure" type II AGN galaxies. With data on infrared PAH features, we found strong correlations between the PAH 11.3/7.7 ratio and the optical narrow-emission line ratios [SII]/Hα as well as the 11.3/7.7 ratio and [OI]/Hα, providing possible evidence that small PAH particles are preferably destroyed by the spectrum of radiation from an AGN. We attempt to relate the fraction of PAHs with $D_n(4000)$ by using those two optical narrow-line ratios, which suggests that older host galaxies tend to have larger PAH 11.3/7.7 ratios.

Acknowledgements We would like to thank the anonymous referee for their very professional and useful suggestions in the discussion section. We want to thank Huali Li, Xianmeng Meng, Hao Liu, Hongbo Cai and Yuanfeng Xuan for their help. This work was supported by the National Basic Research Program of China (973 program, Grant No. 2014CB845800) and the National Natural Science Foundation of China (Grant Nos. 11473036, 11203033 and U1331202). The work is based in part on observations made with the *Spitzer* Space Telescope and made use of the NASA/IPAC Extragalactic Database (NED) which is operated by the Jet Propulsion Laboratory, California Institute of Technology, under contract with the National Aeronautics and Space Administration.

References

Ashby, M. L. N., Houck, J. R., & Matthews, K. 1995, ApJ, 447, 545
Bakes, E. L. O., & Tielens, A. G. G. M. 1994, ApJ, 427, 822
Bakes, E. L. O., Tielens, A. G. G. M., & Bauschlicher, C. W., Jr. 2001, ApJ, 556, 501
Baldwin, J. A., Phillips, M. M., & Terlevich, R. 1981, PASP, 93, 5
Bennert, N., Jungwiert, B., Komossa, S., Haas, M., & Chini, R. 2006, A&A, 456, 953
Clavel, J., Schulz, B., Altieri, B., et al. 2000, A&A, 357, 839
Dale, D. A., & Helou, G. 2002, ApJ, 576, 159
Diamond-Stanic, A. M., & Rieke, G. H. 2010, ApJ, 724, 140
Draine, B. T., & Li, A. 2001, ApJ, 551, 807
Draine, B. T., & Li, A. 2007, ApJ, 657, 810
Dudik, R. P., Satyapal, S., & Marcu, D. 2009, ApJ, 691, 1501
Galliano, F., Madden, S. C., Tielens, A. G. G. M., Peeters, E., & Jones, A. P. 2008, ApJ, 679, 310
Genzel, R., Lutz, D., Sturm, E., et al. 1998, ApJ, 498, 579
Gordon, K. D., Engelbracht, C. W., Rieke, G. H., et al. 2008, ApJ, 682, 336
Goulding, A. D., & Alexander, D. M. 2009, MNRAS, 398, 1165
Gu, Q., Melnick, J., Cid Fernandes, R., et al. 2006, MNRAS, 366, 480
Heckman, T. M., Crane, P. C., & Balick, B. 1980, A&AS, 40, 295
Ho, L. C., Filippenko, A. V., & Sargent, W. L. W. 1997, ApJS, 112, 315
Houck, J. R., Roellig, T. L., van Cleve, J., et al. 2004, ApJS, 154, 18
Kauffmann, G., Heckman, T. M., Tremonti, C., et al. 2003, MNRAS, 346, 1055
Keel, W. C., Kennicutt, R. C., Jr., Hummel, E., & van der Hulst, J. M. 1985, AJ, 90, 708
Kewley, L. J., Dopita, M. A., Sutherland, R. S., Heisler, C. A., & Trevena, J. 2001, ApJ, 556, 121
Kewley, L. J., Heisler, C. A., Dopita, M. A., et al. 2000, ApJ, 530, 704
Kewley, L. J., Groves, B., Kauffmann, G., & Heckman, T. 2006, MNRAS, 372, 961
LaMassa, S. M., Heckman, T. M., Ptak, A., et al. 2010, ApJ, 720, 786
LaMassa, S. M., Heckman, T. M., Ptak, A., et al. 2012, ApJ, 758, 1
Lumsden, S. L., Heisler, C. A., Bailey, J. A., Hough, J. H., & Young, S. 2001, MNRAS, 327, 459
Nagao, T., Murayama, T., Shioya, Y., & Taniguchi, Y. 2002, ApJ, 575, 721

O'Dowd, M. J., Schiminovich, D., Johnson, B. D., et al. 2009, ApJ, 705, 885
Pereira-Santaella, M., Alonso-Herrero, A., Rieke, G. H., et al. 2010, ApJS, 188, 447
Roussel, H., Sauvage, M., Vigroux, L., & Bosma, A. 2001, A&A, 372, 427
Sales, D. A., Pastoriza, M. G., & Riffel, R. 2010, ApJ, 725, 605
Seth, A., Agüeros, M., Lee, D., & Basu-Zych, A. 2008, ApJ, 678, 116
Shi, Y., Rieke, G. H., Smith, P., et al. 2010, ApJ, 714, 115
Shields, J. C., Rix, H.-W., Sarzi, M., et al. 2007, ApJ, 654, 125
Smith, J. D. T., Armus, L., Dale, D. A., et al. 2007a, PASP, 119, 1133
Smith, J. D. T., Draine, B. T., Dale, D. A., et al. 2007b, ApJ, 656, 770
Stasińska, G. 1984, A&A, 135, 341
Storchi-Bergmann, T., Kinney, A. L., & Challis, P. 1995, ApJS, 98, 103
Storchi-Bergmann, T., Schmitt, H. R., Calzetti, D., & Kinney, A. L. 1998, AJ, 115, 909
Tielens, A. G. G. M. 2008, ARA&A, 46, 289
Tran, H. D. 2003, ApJ, 583, 632
Vaceli, M. S., Viegas, S. M., Gruenwald, R., & de Souza, R. E. 1997, AJ, 114, 1345
Veilleux, S., & Osterbrock, D. E. 1987, ApJS, 63, 295
Verma, A., Charmandaris, V., Klaas, U., Lutz, D., & Haas, M. 2005, Space Sci. Rev., 119, 355
Veron-Cetty, M.-P., & Veron, P. 1986, A&AS, 66, 335
Voit, G. M. 1991, ApJ, 379, 122
Voit, G. M. 1992, MNRAS, 258, 841
Wang, J., & Wei, J. Y. 2008, ApJ, 679, 86
Wang, J., & Wei, J. Y. 2010, ApJ, 719, 1157
Wang, J., Zhou, X. L., & Wei, J. Y. 2013, ApJ, 768, 176
Winter, L. M., Lewis, K. T., Koss, M., et al. 2010, ApJ, 710, 503
Wu, Y., Helou, G., Armus, L., et al. 2010, ApJ, 723, 895
Wu, Y.-Z., Zhao, Y.-H., & Meng, X.-M. 2011, ApJS, 195, 17
Yu, P.-C., Huang, K.-Y., Hwang, C.-Y., & Ohyama, Y. 2013, ApJ, 768, 30
Yu, P.-C., & Hwang, C.-Y. 2011, AJ, 142, 14